

Dear reviewer

Please check our response to your comments point-by-point. And the changes track and revised figure were attached behind.

Thanks a lot,
Jianjun Xu

Response to Referee#2

General comments

Although the manuscript addresses relevant scientific questions, the authors not clearly indicate their own new/original contribution respect to the mentioned references/studies. The novelty against the past should be emerged already in the introduction which is the “business card” of the paper. I appreciate the authors effort of adding more literature, but It would be useful to describe more in details results and improvements reached in these studies (**for example pag.6441, lines 5-8**) trying to make more rich and robust this part. Also the final discussion needs a deep revision focusing the attention on substantial conclusions reached and efforts to be done in the future to improve the results. Finally, the language is not always fluent and precise. I also suggest that the manuscript is read by a native speaker or undergoes professional language editing before being published.

Answer: Actually, there is a lot of introduction usin previous studies. For example, Derber J. C. and W-S Wu. 1998: The use of TOVS cloud-cleared radiances in the NCEP SSI analysis system. *Mon. Wea. Rev.*, **126**, 2287–2299.

In order to avoid duplication, we only simply gave a short summary. Different from the previous studies, we focus on the different impacts of hyperspectral infrared and microwaves radiance data assimilation on the weather forecasts, especially on the different performance of vertical structures.

Specific comments

Pag. 6442, lines 16-18 >> Try to better explain the usefulness of outer iterations and why you choose two and not more outer iterations.

Answer: The experiment design is based on the suggestion of John Deber's report, actually the two outer iterations are used in NOAA operational forecasts, which has been verified in the operational forecasts.

Pag. 6444, line 2 >> “with an initial time at 18:00 UTC” >> of which day?

Answer: The sentence has been changed to “with an initial time at 18:00 UTC of 30 June to 30 July”

Pag. 6444, line 3 >> which is the second control experiment?

Answer: In order to avoid the confusion, We changed the word 'second' to "continued".

Actually the second control experiment means continuing to the first control experiment from 00:00 UTC. The first run initiated from 18:00 UTC and integrated 6 hours. Then the continued run from 00:00 UTC.

Pag. 6444, lines 13-18 >> please add related literature of the physics schemes
Answer: Done.

Pag. 6444, lines 21-23 >> please add the source of conventional observations
Answer: We give the source of conventional observations in the revised version.

Pag. 6445, lines 5-6 >> please say when these coverage is refer to, as stated in the caption of figure 1b
Answer: We have added the reference times for the radiances in the new version.

Pag. 6447, line 10 >> please change the title in something like “Impact of DA on....”
Answer: Done.

Pag. 6450, line 1 >> please change the title in something like “Impact of DA on....”
Answer: Done.

Pag. 6452, lines 9-10 >> Try to better explain the statement “The reason is very complicated, it is partially attributed to the data selection in the processes of the data assimilation.”

Answer: It is partially attributed because IASI data has 8461 channels, but we only used 279 channel based on previous studies. Until now, we really don't know what is responsible for the different performances since many factors have contributed to the overall result. More experiments are necessary as part of our future study to try and understand the contributions from the various factors and components used in the analysis..

Pag. 6452, line 19... >> no next steps for the future?

Answer: Actually, we plan to examine longer experiments, using more data channels and more satellite sensors as part of future investigations.

Technical corrections

Pag.6441, line 18 >> highspectralresoluton >> miss the “i”

Response: Done

Pag.6441, line 20 >> please check “most optimal” in english

Response: the word most was removed.

Pag. 6442, line 2 >> please write ARW-WRF always in the same way

Response: Done.

Pag. 6442, line 13 >> “that is from GFS 6h forecast filed in this study” >> that comes from GFS 6h forecast for this study

Response: done.

Pag. 6442,line 19 >> Remove comma after “function,”

Response: done.

Pag. 6442, line 21 >> “contains”

Response: done.

Pag. 6443, line 7 >> Put “:” instead of “.” after “satellite data”

Response: done

Pag. 6443, line 19 >> Remove “through”

Response: done

Pag. 6443, line 23 >> Substitute “to the” with “as the”

Response: done

Pag. 6443, lines 25-26 >> “covered more of the region than at other anytime” >> not so clear, try to say better in english

Response: we have revised this sentence to make it clear.

Pag. 6444, lines 78 >> too many repetitions of “only”

Response: yes, the only has been deleted

Pag. 6444, line 14 >> “Yosei” >> Yonsei

Response: done

Pag. 6444, line 18 >> Pa or hPa ?

Response: done

Pag. 6444, line 25 >> “most of the atmospheric”

Response: done

Pag. 6445, line 1 >> “the most WSP data” >> most of the WSP data

Response: done

Pag. 6445, line 7 >> “In this study the channels from 4 to 14 are assimilated...”

Response: done

Pag. 6445, line 9 >> substitute “by Fig. 2a” with “in Fig. 2a”

Response: done

Pag. 6445, line 12 >> substitute “by Fig. 2b” with “in Fig. 2b”

Response: done

Pag. 6445, lines 13-18 >> too many repetitions of “can detect” >> please find synonymous

Response: done

Pag. 6445, line 22 >> remove the first “i” in “huimidity”

Response: done

Pag. 6445, line 23 >> remove comma before “and”

Response: done

Pag. 6445, line 25 >> substitute “by Fig. 2c” with “in Fig. 2c”

Response: done

Pag. 6445, line 27 >> please define the acronym NESDIS

Response: done

Pag. 6446, line 3 >> “ingested into the data assimilation system”

Response: done

Pag. 6446, line 8 >> “Previous publications.....” >> this period is not clear

Response: delete ' Previous publications '

Pag. 6446, line 11 >> please add a reference for GDAS and define the acronym

Response: done

Pag. 6446, line 11 >> “ and it can be used to correct...”

Response: done

Pag. 6446, line 12 >> “To that purpose in this study...”

Response: done

Pag. 6446, lines 15-16 >> “surface pressure (Fig. 3a), atmospheric temperature at the height of 2m (Fig. 3b) and wind speed at the height of 10m (Fig. 3c)”

Response: [done](#)

Pag. 6447, line 6 >> “error” >> “errors”

Response: [done](#)

Pag.6447, line 12 >> “The three involved...”

Response: [done](#)

Pag.6447, line 13 >> “show” instead of “showing”

Response: [done](#)

Pag.6447, line 13 >> “For the first 24 hours it seems that...”

Response: [done](#)

Pag.6448, line 4 >> “within” instead of “with”

Response: [done](#)

Pag.6448, line 5 >> “give” instead of “make”

Response: [done](#)

Pag.6448, line 9 >> “gave” instead of “made”

Response: [done](#)

Pag.6449, line 4 >> “and it” instead of “and the RMS error”

Response: [done](#)

Pag.6449, line 20 >> “gave” instead of “made”

Response: [done](#)

Pag.6449, line 21 >> “gives” instead of “makes”

Response: [done](#)

Pag.6449, line 23 >> “impact” instead of “contribution”

Response: [done](#)

Pag.6450, line 7 >> “different” instead of “differing”

Response: [done](#)

Pag.6450, line 7 >> “in the entire troposphere”

Response: [done](#)

Pag.6450, line 18 >> “gave” instead of “made”

Response: [done](#)

Pag.6451, line 6 >> “forecasts: in fact, the RMS error profile...”

Response: [done](#)

Pag.6451, line 9 >> “gave” instead of “made”

Response: [done](#)

Pag.6451, lines 9-10 >> “has a negative impact on the ...”

Response: [done](#)

Pag.6451, line 18 >> “give” instead of “make”

Response: [done](#)

Pag.6451, line 22 >> “linked to” instead of “linkage with”

Response: [done](#)

Pag.6451, lines 22-28 >> This period is too long!

Response: [yes, we have changed the sentence](#)

Pag.6452, lines 6-7 >> “For the humidity forecast there is a different behavior: the IASI data...”

Response: [done](#)

Pag.6452, line 11 >> “showed” instead of “shown”

Response: [done](#)

Pag.6452, line 11 >> “the partial impact of ” instead of “the some impacts of”

Response: [done](#)

TABLES & FIGURES

It would be useful to add the “initial time” of each experiment of Table 1

Caption of figures 57910 >> “Other definitions are the same of Fig.4”

Caption of figures 68 >> “Other definitions can be found in Table 1”

Response: [yes, please check these Figures and table.](#)

1 **Abstract**

2 Using NOAA's Gridpoint Statistical Interpolation (GSI) data assimilation system and
3 NCAR's Advanced Research WRF (ARW-WRF) regional model, six experiments are designed
4 by (1) control experiment (CTRL) and five data assimilation (DA) experiments with different
5 data sets including (2) conventional data only (CON), (3) microwave data (AMSU-A + MHS)
6 only (MW), (4) infrared data (IASI) only (IR), (5) s combination of microwave and infrared data
7 (MWIR), and (6) a combination of conventional, microwave and infrared observation data
8 (ALL). One month experiments in July 2012 and the impacts of the DA on temperature and
9 moisture forecasts at the surface and four vertical layers, ~~which~~ over the western United States
10 have been investigated. The four layers include lower troposphere (LT) from 800 to 1000 hPa,
11 middle troposphere (MT) from 400 to 800 hPa, upper troposphere (UT) from 200 to 400 hPa and
12 lower stratosphere (LS) from 50 to 200 hPa. The results show that the regional GSI/WRF system
13 is underestimating the observed temperature in the LT and overestimating in the UT and LS. The
14 MW DA reduced the forecast bias from the MT to the LS within 30-hour forecasts, and the CON
15 DA kept a smaller forecast bias in the LT for 2-day forecasts. The largest RMS error is observed
16 in the LT and at the surface (SFC). Compared to the CTRL, the MW DA made the most positive
17 contribution in the UT and LS, and the CON DA mainly improved the temperature forecasts at
18 the SFC. However, the IR DA made a negative contribution in the LT.

19 Most of the observed humidity in the different vertical layers is overestimated in the
20 humidity forecasts except in the UT. The smallest bias in the humidity forecast occurred at the
21 SFC and UT. The DA experiments apparently reduced the bias from the LT to UT, especially for
22 the IR DA experiment, but the RMS errors are not reduced in the humidity forecasts. Compared
23 to the CTRL, the IR DA experiment has a larger RMS error in the moisture forecast although the

1 smallest bias is found in the LT and MT.

2 Key words: Data assimilation, temperature, humidity, forecast

3

4

5

6

7

8

9

10

11

12

13

14

15

16

17

18

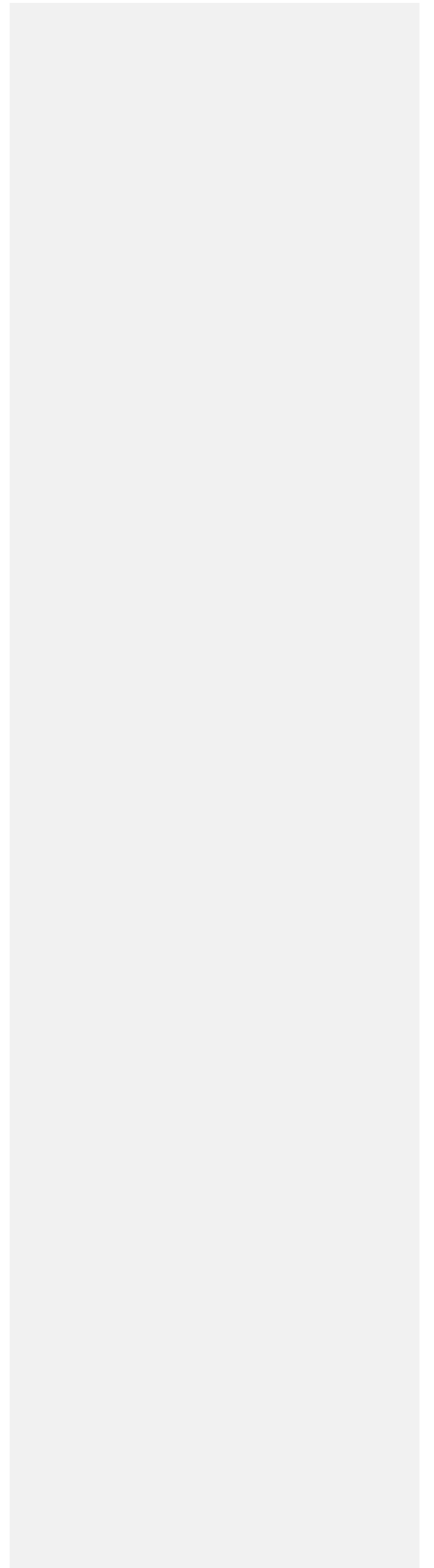
19

20

21

22

23



1 1. Introduction

2 Instead of ~~a~~the random distribution and heterogeneous spatial density in the traditional
3 conventional radiosondes, satellite observations provide a large amount of data covering
4 worldwide areas for improving the initialization of the weather forecasts models through a data
5 assimilation system. Many studies demonstrated that the assimilation of satellite data
6 significantly improved weather forecasts (Eyre 1992; Andersson et al. 1991; Derber and Wu
7 1998; Zhou et al. 2011), especially over some areas with sparse conventional observations
8 (McNally et al. 2000; Zapotocny et al. 2008; Liu et al., 2012)

9 The Meteorological Operational satellite program (MetOp) launched its first polar orbiting
10 satellite (MetOp-A) on October 19, 2006. MetOp-A is in a sun-synchronous orbit, carrying a
11 payload of 10 scientific instruments including the Advanced Microwave Sounding Unit-A
12 (AMSU-A), Microwave Humidity Sounder (MHS) and the new generation Infrared Atmospheric
13 Sounding Interferometer (IASI) to make atmospheric soundings at various altitudes. IASI
14 (Clerbaux, et al. 2009) measures the radiance emitted from the Earth in 8461 channels covering
15 the spectral interval 645-2760 cm^{-1} at a resolution of 0.5 cm^{-1} (apodized) and with a spatial
16 sampling of 18 km at nadir. Limited spectral data is currently transmitted, stored and assimilated.
17 Rabier et al. (2002) compared a number of techniques for channel selection from high-spectral-
18 resolution infrared sounders, and concluded that the channel-selection method of Rodgers (1996,
19 2000) is the ~~most~~-optimal method. Collard (2007) applied his method to select a subset of 300
20 channels for data assimilation, so that the total loss of information for a typical numerical
21 weather prediction (NWP) state vector consisting of one or more of temperature, humidity is
22 minimized.

23 This study focuses on assessing the effects of AMSU-A, MHS and IASI data assimilation

1 on numerical weather forecasts over the western United States. The model, data and
2 methodology are presented in the section 2 and section 3, respectively. Section 4 describes the
3 results of experiments. The results are summarized and discussed in section 5.

4 **2. Model**

5 **2.1 The GSI system for ARW-WRF Regional Model**

6 The assimilation system used here is the Gridpoint Statistical Interpolation (GSI) analysis
7 system, which is developed by United States National Centers for Environmental Prediction
8 (NCEP). The current GSI regional analysis system accepts NCEP's Nonhydrostatic Mesoscale
9 Model (NMM) WRF and NCAR's Advanced Research WRF (ARW) WRF mass core (Liu and
10 Weng, 2006; Xu and Powell, 2011; Wan and Xu, 2011). The interfaces are specialized
11 separately for the WRF NMM core and the WRF ARW core. The analysis system produces an
12 analysis through the minimization of an objective function given by

$$13 \quad J = \frac{1}{2}(x - x^b)^T B^{-1}(x - x^b) + \frac{1}{2}(H(x) - y^o)^T R^{-1}(H(x) - y^o)$$

14 Where x is the analysis state, B is the background error covariance matrix, x^b is the first guess
15 that is comes from GFS 6-h forecast field led in this study, H is the transformation operator from
16 the analysis variable to the form of the observations, y^o is the observation such as AMSU-A,
17 MHS, IASI, etc.

18 The minimization algorithm is composed of two outer iterations to account for weak
19 nonlinearities in the cost function. In the first external iteration the first guess is a 6-h forecast,
20 while in the second one it is the solution from the previous outer iteration. In the cost function,
21 B has been estimated from scaled differences between 24-h and 48-h forecasts valid at the same
22 time (Parrish and Derber, 1992). The observation error covariance matrix (R) contains
23 information on the observational error and errors in representativeness, which has been

1 calculated before running the GSI.

2 **2.2 Radiative Transfer Model**

3 The radiative transfer model incorporated into the GSI data assimilation system at the
4 NCEP is the Community Radiative Transfer Model (CRTM). The CRTM was developed by the
5 ~~United States~~ Joint Center for Satellite Data Assimilation (JCSDA) for rapid calculations of
6 satellite radiances based on radiative transfer (RT) theory (Han, et al. 2006). The forward model,
7 tangent-linear, adjoint and K-matrix models were also developed for ~~the~~ data assimilation of
8 satellite data. CRTM is always updated for new satellite data. It supports a large number of
9 sensors onboard geostationary and polar-orbiting satellites, covering the microwave, infrared and
10 visible frequency regions.

11 The CRTM comprises four major modules: (1) RT solution module, (2) atmospheric
12 transmittance module, (3) surface emissivity/reflectivity module, (4) particle scattering module.
13 Six RT solution schemes were tested in the CRTM (Weng et al., 2007). According to several
14 performance factors, the advance doubling and adding scheme (ADA; Liu and Weng, 2006) was
15 selected for the CRTM implementation. In CRTM, a fast and optimal spectral sampling (OSS)
16 absorption model (Moncet et al. 2004) is used to calculate atmospheric transmittance.

17 **2.3 Experiment Design**

18 The objective of this study is to explore the effect of satellite data assimilation on the main
19 atmospheric state forecast ~~throughby~~ -comparing the results from microwave (AMSU-A and
20 MHS), hyperspectral infrared radiance (IASI) and conventional data assimilation. Over the main
21 continent of United States of America (USA), there are many conventional observation stations,
22 which can be used to validate the forecast results. Therefore, the western coast region of the USA
23 is selected ~~to as~~ the experimental region. ~~Analyzing the satellite data (AMSU-A, MHS and IASI)~~

1 ~~covering the western USA at 00, 06, 12 and 18 UTC, the satellite data at 18 UTC covered more~~
2 ~~of the region than at other anytime. There were more satellite data coverage of the experimental~~
3 ~~region around 18 UTC than other time, such as 00, 06, 12 and 18 UTC.~~ The covered region at
4 18 UTC is 20° - 55°N and 85° - 155°W, which includes the western USA and sea area near the
5 west coast (Figure 1).

6 The experiment design includes six simulations (Table 1). The control (CTRL) experiment
7 is first made with an initial time at 18:00 UTC ~~of~~from 30 June to 30 July and makes 6-h forecasts.
8 The five data assimilation (DA) experiments and the continued ~~second~~-control experiment are
9 made with initial time at 00:00 UTC from July 1 to 31, 2012 and make a 72-h forecast for each
10 day. The initial condition in all six experiments is obtained from the 6-h forecasts of the first
11 control experiment. The five DA experiments are made with different data sets including
12 conventional data ~~only~~-(CON), microwave data (AMSU-A + MHS) ~~only~~-(MW), infrared data
13 (IASI) ~~only~~-(IR), a combination of microwave and infrared data (MWIR), a combination of
14 conventional, microwave and infrared observation data (ALL). The initial condition and lateral
15 boundary conditions came from the operational GFS forecast at 6-h intervals and 0.5 x 0.5
16 degree resolution, which were downloaded from NCEP data inventory
17 (<ftp://ftp.ncep.noaa.gov/pub/data/nccf/com/gfs/prod/>).

18 In the ARW model, the physics of the model includes the Goddard Cumulus Ensemble
19 (GCE) microphysics scheme, Yonsei University planetary boundary layer (PBL) scheme, Noah
20 land surface model, Rapid Radiative Transfer Model (RRTM) longwave radiation, and the
21 Goddard shortwave radiation scheme ([Xu et al., 2009](#)). The 15-km WRF model forecast with a
22 mesh size domain of 718 X 373 (Fig.1) was used. Forty-three (43) vertical layers were selected
23 for use with a model top of 10 hPa.

1 **3. Data and Methodology**

2 **3.1 Conventional and Satellite data**

3 In this study, the conventional observation data includes atmospheric temperature (T),
4 moisture (Q) and wind speed (WSP) at various pressure levels and pressure data at the surface
5 [that were downloaded from NCEP data inventory \(ftp://ftp.ncep.noaa.gov/pub/data/
6 nccf/com/gfs/prod/\)](ftp://ftp.ncep.noaa.gov/pub/data/nccf/com/gfs/prod/). Figure 1a shows the distribution of the conventional data on July 1, 2012
7 where the atmospheric temperature, moisture and surface pressure observations are rare. Most of
8 atmospheric temperature and moisture observations are conducted at the surface level in [the](#)
9 pressure range of 1000-1200 hPa. ~~Most of the~~ [The most](#) WSP data are found over the sea close to
10 the [western](#) coast of ~~western-the~~ United States.

11 The satellite data includes the Advanced Microwave Sounding Unit-A (AMSU-A),
12 Microwave Humidity Sounder (MHS) and the new generation Infrared Atmospheric Sounding
13 Interferometer (IASI). Figure 1b shows the distribution of the AMSU-A, MHS and IASI datasets
14 [acquired about at 18:00 UTC on July 1, 2012](#). AMSU-A is a 15-channel cross-track, stepped-line
15 scanning, total power microwave radiometer. ~~In this study the~~ channels from 4 to 14 are
16 assimilated ~~in this study~~, which were designed to detect atmospheric temperature at 11 layers
17 from the surface to around 45 km. Their weighting function is illustrated ~~in by~~ Figure 2a. MHS
18 on the other hand probes at millimetric frequencies between 89 and 183 GHz, the channels from
19 2 to 5 are assimilated, which were designed to detect atmospheric moisture at 2 layers from
20 surface to around 400 hPa. Their weighting function is illustrated ~~in by~~ Figure 2b. Channel 4 of
21 AMSU-A and channel 2 of MHS can detect the atmospheric temperature and humidity at the
22 lowest layer of the troposphere. Channels 5 and 6 of AMSU-A and channels 3, 4 and 5 of MHS
23 can ~~represent~~ [detect](#) the atmospheric temperature and humidity in the middle atmospheric layer of

1 | the troposphere. Channel 7 of AMSU-A can ~~indicate~~ detect the atmospheric temperature in the
2 | highest layer of troposphere. Channels 9 and 10 of AMSU-A can detect the atmospheric
3 | temperature in lower layer of the stratosphere

4 | The IASI instrument covers the spectral range from the thermal infrared at 3.62 μm (2760
5 | cm^{-1}) to 15.5 μm (645 cm^{-1}) covering the peak of the thermal infrared and particularly the CO2
6 | band with the humidity (Q) branch around 666 cm^{-1} . Within these bands, the selected 279 bands
7 | (Table 2) correspond to atmospheric temperature and humidity. A band number smaller than
8 | 515 represents atmospheric temperature, and a band number larger than 2701 represents
9 | atmospheric humidity. Their weighting function is illustrated ~~in~~ by Figure 2c.

10 | 3.2 Radiance data quality control and bias correction

11 | The radiance data have been preprocessed by [NOAA's Satellite and Information Service](#)
12 | [\(NESDIS\)](#) before becoming available for usage. The data have been statistically limb corrected
13 | (adjusted to nadir) and surface emissivity corrected in the microwave channels and cloud cleared
14 | in the tropospheric channels. Although the satellite data have undergone preprocessing, they
15 | need further bias correction before being ingested into data assimilation system. The source of
16 | the biases can be related to instrument calibration problems, and predictor and zenith angle bias.
17 | It was demonstrated that a successful bias correction scheme must take into account the spatially
18 | varying and air-mass dependent nature of radiance biases. ~~Previous publications have~~ (Kelly and
19 | Flobert, 1988; McMillin et al., 1989; Uddstrom, 1991). Eyre (1992) and Harris and Kelly
20 | (2001) categorized the bias into two types: scan bias and air-mass bias, and presented a bias
21 | correction scheme. GSI uses this bias correction scheme to correct radiance bias. The radiance
22 | bias correction coefficients ~~might~~ may be downloaded from [Global Data Assimilation System](#)
23 | [\(GDAS\)](#) ~~(define GDAS)~~ data directory (<ftp://ftp.ncep.noaa.gov/pub/data/nccf/com/gfs/prod/>).

1 and it can be used to correct the radiance bias in GSI. To that purpose in this study, monthly
2 regional mean innovations, e.g. observation minus background (OMB) and observation minus
3 analysis (OMA), are calculated with or without bias corrections in this study. For example, Fig.
4 ~~ure-3 is shows~~ the scattering plots of surface pressure (Fig. 3a), atmospheric temperature at the
5 height of 2m (Fig. 3b)~~2-meters~~ and wind speed at the height of 10m (Fig. 3c)~~10-meters~~ between
6 OMB and OMA in the ALL data experiment. The result shows that the slope of the simulated
7 line is less than 1, which indicates the analysis fields are closer to observation than background
8 fields.

9 **3.3 Methodology**

10 In order to evaluate the effects of radiance data assimilation on temperature and moisture
11 at the different vertical layers, the surface (SFC) and four atmospheric layers are examined. The
12 four layers include lower troposphere (LT) from 800 to 1000 hPa, middle troposphere (MT) from
13 400 to 800 hPa, upper troposphere (UT) from 200 to 400 hPa and lower stratosphere (LS) from
14 50 to 200 hPa. Similar to ~~the a~~ previous study (Xu, et al., 2009), two statistical variables - bias
15 and root mean square (RMS) errors s are investigated.

16 If X represents any of the parameters under consideration for a given time and vertical level,
17 then the forecast error is defined as $X' = X_f - X_o$ where the subscripts f and o denote forecast and
18 observed quantities, respectively. Given N valid pairs of forecasts and observations, the bias is
19 computed as

$$20 \quad bias = \overline{X'} = \frac{1}{N} \sum_{i=1}^N X'_i \quad (1)$$

21 the root mean-square (RMS) error is computed as

$$22 \quad RMS = \sqrt{\frac{1}{N} \sum_{i=1}^N (X'_i)^2} \quad (2)$$

1 The bias and RMS error at 00:00 and 12:00 UTC are calculated because more than enough
2 observational data and approximately 3000 sounding stations can be used at the two times.

3 **4. Results**

4 **4.1 Impact of DA on Temperature**

5 At the SFC, the CON (conventional data only) DA experiment shows (Fig.4a) the smallest
6 bias value in all six experiments. ~~The three involved~~ infrared satellite DA experiments
7 (IR, IR+MW, IR+MW+CON) showing a larger bias than the CTRL experiment. ~~For the first 24~~
8 ~~hours, it~~ seems that satellite radiance DA, especially for the infrared IASI data, make a negative
9 contribution to the temperature forecasts. ~~Interestingly~~ ~~In additon~~, the bias characterized a
10 diurnal cycle feature for the 72-h forecasts, with the smaller bias appearing at 06, 30, 54 and 72-h
11 corresponding to a local time at 4:00 pm while the higher bias appeared at 18, 42 and 66-h
12 corresponding to 4:00 am local time.

13 Compared to the SFC, the LT shows a more clear diurnal variation (Fig. 4b), and all model
14 forecasts underestimated the observed temperature. The CTRL and CON experiments obtained
15 the smallest forecast bias.

16 Different from the SFC and LT, the diurnal variation of bias disappeared in the MT (Fig.
17 4c). Compared to the CTRL experiment, the bias is significantly reduced in all DA experiments
18 especially for the two combination experiment (MWRI and ALL), the bias is almost zero with ~~in~~
19 the 30-h forecast. It implies that both MW (AMUS-A and MHS) and IR (IASI) DA ~~make-give~~ a
20 positive contribution to the accuracy of temperature forecasts at the MT.

21 At the UT, the smaller bias appeared ~~at-in~~ the CON and MW DA experiments (Fig. 4d), and
22 the combination DA experiments (MWIR and ALL) show a larger bias than the CTRL
23 experiment. The results indicate that the IR DA ~~made~~ a negative contribution to the

1 temperature forecasts and the MW experiment improved the forecast accuracy in the UT.

2 | In contrast, the bias in the LS indicates an opposite pattern to the SFC and LT ~~that~~ where
3 all satellite DA experiments reduced the forecast bias (Fig. 4e). The result demonstrated that the
4 | conventional DA did not improve the forecasts because of the sp~~r~~arse observational data used in
5 this layer. The MW DA obtained the smallest bias ~~at~~ in the LS.

6 | In order to clearly understand the different performance in the six experiments, the
7 temperature forecast bias profile at 6-h, 30-h and 54-h has been examined. Fig. 5 indicates a
8 similar pattern at the three forecast times where the lower bias can be found at the SFC and MT
9 while the larger bias appeared at the UT and LS. Generally, the model forecasts overestimated
10 the observed temperature except in the LT. Compared to the CTRL experiment, the four satellite
11 DA experiments (MW, IR, MWIR and ALL) show a smaller bias from the MT through LS, but
12 the forecasts did not get improved in the LT below 800 hPa. In contrast, the CON experiment has
13 better performance in the LT, especially at the SFC.

14 | It is obvious that the larger bias in temperature forecast appeared in the LT, UT and LS, but
15 the model is underestimating the observed temperature in the LT and overestimating in the UT
16 and LS (Fig. 5). The satellite DA, especially for the MW DA experiment using AMSU-A,
17 | reduced the forecast bias at the levels from the MT to LS. Meanwhile, the CON DA has a
18 smaller forecast bias in the LT, especially at the SFC. Note the IR experiment using the IASI
19 data produced a worst result in the LT.

20 | The forecast RMS error demonstrated some different features (Fig. 6). First, the RMS error
21 | reduced the diurnal variation and ~~the RMS error~~ it significantly increased with the extended
22 length of forecast time at the SFC. The RMS error in the CON and MW experiments is slightly
23 less than that in the CTRL experiment and the other three satellite DA experiments within 24-h

1 forecasts (Fig. 6a). Second, consistent with the larger negative bias in all the satellite DA
2 experiments (Fig. 4b) in the LT, larger RMS errors are observed in these DA experiments (Fig.
3 6b) compared to the CTRL. Third, different from the smaller bias in the DA experiments, the
4 larger RMS errors are maintained in the DA experiments in the MT (Fig. 6c). Fourth, the CON
5 and MW experiments improved the temperature forecasts in the UT (Fig. 6d). But in the LS, the
6 ~~involved~~ microwave DA experiments including MW, MWIR and ALL indicate ~~the~~ smaller RMS
7 errors than the CTRL experiments (Fig. 6e). It is apparent that the CON DA ~~made-gave~~ a
8 negative contribution to the temperature forecast in the LS.

9 Corresponding to the bias profile (Fig. 5), the forecast RMS error profile at 6-h, 30-h and
10 54-h indicates (Fig. 7) that the smallest RMS error is observed at the MT and the largest RMS
11 error appeared in the LT and SFC. Compared to the CTRL experiment, the smaller RMS errors
12 are only found in the MW experiment in the UT and LS, and the CON DA made a positive
13 contribution at the SFC and UT.

14 The results clearly show the IR DA experiment ~~makes-gives~~ a negative contribution to the
15 temperature forecast in the regional system. But the MW DA experiment shows a positive
16 ~~impacted~~ contribution at the LS, and the CON experiment displays better performance at the SFC
17 and UT. It is worth noticing that the RMS error is not always consistent with the bias in the
18 temperature forecasts, for example, the smaller bias appeared at the SFC while a larger RMS
19 error is observed there.

20 **4.2 Impact of DA on hHumidity**

21 Similar to the temperature forecasts at the SFC, the diurnal variation of the moisture bias is
22 observed and the smallest bias appeared in the CON and CTRL experiments within the 42-h
23 forecast (Fig. 8a) with largest bias occurring in the MWIR experiment at 18-h. It is clear that all

1 four satellite DA experiments do not improve the moisture forecast compared to the CTRL
2 experiment. In contrast, the IR DA produced a larger bias significantly differ~~ent~~^{ing} from the
3 other experiments in the entire troposphere (Fig. 8b,c,d). It seems to tell us that the IR DA
4 significantly impacts the humidity forecasts in the troposphere. However, the impacts
5 disappeared in the LS (Fig. 8e).

6 Compared to the bias profile of the temperature forecast (Fig 4), all model runs
7 overestimated the observed humidity except for the UT. The smallest bias in the humidity
8 forecast occurred at the SFC and UT (Fig. 9). Most of DA experiments apparently reduced the
9 bias from LT to UT, especially for the IR experiment. But it is worth noting that the MW DA
10 has a larger bias than the CTRL experiment in the whole troposphere.

11 However, the RMS error in the humidity forecasts (Fig. 10) increases from the SFC to LS.
12 The largest error in the UT and LS is almost double the amount at the SFC. In addition, most of
13 DA experiments demonstrated a larger RMS error than that in the CTRL experiment. In other
14 words, the DA experiments ~~made-gave~~ a negative contribution to the humidity forecasts. The IR
15 DA experiment did not improve moisture forecast although its bias is very small at the LT and
16 MT.

17 **5. Summary and Discussion**

18 **5.1 Summary**

19 In this study, six experiments were designed to assess the effects of data assimilation on
20 atmospheric temperature and moisture forecasts over the western United States. The results are
21 summarized as follows.

22 The regional model underestimates the observed temperature in the LT and overestimates
23 it in the UT and LS. The MW experiment reduced the forecast bias from the MT to LS, and the

1 CON DA obtained a smaller forecast bias in the LT, especially at the SFC. But the IR
2 experiment using the IASI data obtained the largest bias in the LT.

3 However, the RMS error is not always consistent with the bias profile in the temperature
4 forecasts. ~~in fact,~~ the RMS error profile shows that the largest RMS error appeared in the LT
5 and the smallest error in the MT. Compared to the CTRL experiment, the smaller RMS errors are
6 only found in the MW experiment in the UT and LS, and the CON DA ~~made-gave~~ a positive
7 contribution at the SFC and in the UT. The IASI DA experiment ~~hasmade~~ a negative
8 ~~impacted contribution onto~~ the temperature forecast in the regional forecast system.

9 In contrast, all model forecasts overestimated the observed humidity except in the UT. The
10 smallest bias in the humidity forecast occurred at the SFC and in the UT. Most of DA
11 experiments apparently reduced the bias in the LT to UT, especially for the IR DA experiment.
12 But the MW DA obtained a larger bias than the CTRL experiment in the entire troposphere.

13 The RMS error in the humidity forecasts increases from the SFC to the LS, which is similar
14 to the bias profile except in the UT. The largest error in the UT and LS is almost double the
15 amount at the SFC. The DA experiments ~~make-give~~ a limited contribution to the humidity
16 forecasts. The IR DA experiment does not improve the moisture forecast although its smallest
17 bias is found in the LT and MT.

18 5.2 Discussion

19 This is a study using WRF-ARW mesoscale model ~~linked to linkage with~~ GSI data
20 assimilation system to explore the impacts of AMSU-A/MHS and IASI radiance data
21 assimilation on the temperature and humidity forecasts in the different vertical layers over the
22 western coast of United States, due to the complexity of measurements for satellite instruments
23 (such as IASI has 8461 channels) and lack of knowledge in the estimation of impacts of those

1 | datasets in this regional area, forecasters should be aware of the limitations of these data
2 | assimilation when forecasting in this region.

3 | The results show that the bias and forecast error is substantially related to the vertical
4 | layer of the objective. For example, the AMSU-A data assimilation -reduced the temperature
5 | forecast bias in the upper atmospheric layers, the conventional data assimilation indicates the
6 | best performance in the lower layer, but the IASI data assimilation shows worst performance in
7 | the lower layer. Compared to the largest bias in the upper atmospheric layer, the largest RMS
8 | error appeared in the lower atmospheric layers. ~~For the~~ The humidity forecast ~~there is a~~ different
9 | ~~behavior~~; the IASI data assimilation significantly reduced the bias in the troposphere, but the
10 | RMS error tells us that the IASI data assimilation does not improve the moisture forecast in this
11 | layer. The reason is very complicated, it is partially attributed to the data selection in the
12 | processes of the data assimilation. The results show~~ed~~ in this analysis demonstrate the
13 | ~~partial~~~~some~~ impacts of satellite data on temperature and humidity forecasts in this region, but the
14 | positive or negative impact depends on the atmospheric layer and forecasts variables.

15 | It is worth noting that the results presented here are based on one month's forecasts with
16 | three satellite instruments. The model performance needs to be examined with longer
17 | experiments and more data selection that extend to all available satellite data sets and more
18 | experiments from the different areas. As expressed by Manning and Davis (1997), "These
19 | statistics would provide additional information to model users and alert model developers to
20 | those research areas that need more attention."

21 | ***Acknowledgements.***

22 | The GSI data assimilation system was obtained from Joint Center for Satellite Data Assimilation
23 | (JCSDA), WRF-ARW model was obtained from the NCAR, the satellite datasets were provided

1 by NOAA/NESDIS/STAR. The authors would like to thank these agencies for the model and
2 data providing. This work was partially supported by a project funded by the Priority Academic
3 Program Development of Jiangsu Higher Education Institutions (PAPD), the National Natural
4 Science Foundation of China (No. 40701130), the No-for-Profit Industry (Meteorology)
5 Research Program, China (GYHY201106027), and Jiangsu Key Laboratory of Meteorological
6 Observation and Information Processing (S5311026001) at the Nanjing University of
7 Information Science and Technology, Nanjing, China.

8 This work was partially supported by the National Oceanic and Atmospheric Administration
9 (NOAA), National Environmental Satellite, Data, and Information Service (NESDIS), Center for
10 Satellite Applications and Research (STAR). The views, opinions, and findings contained in this
11 publication are those of the authors and should not be considered an official NOAA or U.S.
12 Government position, policy, or decision.

13 **Reference**

14 Andersson, E., A. Hollingsworth, G. Kelly, P. Lönnberg, J. Pailleux, and Z. Zhang, 1991: Global
15 observing system experiments on operational statistical retrievals of satellite sounding
16 data. *Mon. Wea. Rev.*, **119**, 1851–1864.

17 Clerbaux C., A. Boynard , L. Clarisse , M. George , J. Hadji-Lazaro , H. Herbin , D. Hurtmans ,
18 M. Pommier, A. Razavi , S. Turquety, C. Wespes and P.-F. Coheur, 2009: Monitoring
19 of atmospheric composition using the thermal infrared IASI/MetOp sounder. *Atmos.*
20 *Chem. Phys.*, 9, 6041– 6054, 2009. www.atmos-chem-phys.net/9/6041/2009/

21 Collard AD. 2007. Selection of IASI channels for use in numerical weather prediction. *Q. J. R.*
22 *Meteorol. Soc.* **133**: 1977–1991

23 Derber J. C. and W-S Wu. 1998: The use of TOVS cloud-cleared radiances in the NCEP SSI

1 analysis system. *Mon. Wea. Rev.*, **126**, 2287–2299.

2 Eyre J. A bias correction scheme for simulated TOVS brightness temperatures. Tech. Memo.
3 186, ECMWF (1992).

4 Han Y., Paul van Delst, Q. Liu, F. Weng, B. Yan, R. Treadon and J. Derber, 2006: JCSDA
5 Community Radiative Transfer Model (CRTM) - Version 1, *NOAA Tech Report 122*.

6 Harris B. and Kelly G., A satellite radiance bias correction scheme for data assimilation *Quart. J.*
7 *Roy. Meteorol. Soc.* 127, 1453 (2001).

8 Kelly GA, Flobert JF. 1988. Radiance tuning. In: *Technical Proceedings of the Fourth*
9 *International TOVS Study Conference*, Igls, Austria, 16–22 March 1988: 99–117.

10 Liu Q, Weng F. Detecting the warm core of a hurricane from the Special Sensor Microwave
11 Imager Sounder. *Geophys. Res. Lett.* 2006; 33: L06817, doi:10.1029/2005GL025246.

12 Liu, Q., and F. Weng, 2006: Advanced doubling–adding method for radiative transfer in
13 planetary atmosphere. *J. Atmos. Sci.*, **63**, 3459–3465.

14 Liu, Zhiqian, Craig S. Schwartz, Chris Snyder, and So-Young Ha. "Impact of assimilating
15 AMSU-A radiances on forecasts of 2008 Atlantic tropical cyclones initialized with a
16 limited-area ensemble Kalman filter", *Monthly Weather Review*, 2012.

17 Manning, K. W., and C. A. Davis, 1997: Verification and sensitivity experiments for the
18 WISP95 MM5 forecasts. *Weather Forecasting*, **12**, 719–735

19 McMillin, L. M., L. J. Crone, and D. S. Crosby, 1989: Adjusting satellite radiances by regression
20 with an orthogonal transformation to a prior estimate. *J. Appl. Meteor.*, 28, 969–975.

21 McNally, A. P., J. C. Derber, W. Wu, and B. B. Katz, 2000: The use of TOVS level-1b radiances
22 in the NCEP SSI analysis system. *Quart. J. Roy. Meteor. Soc.*, **126**, 689–724.

23 Moncet, J., G. Uymin, and H. E. Snell, 2004: Atmospheric radiance modeling using the Optimal

1 Spectral Sampling (OSS) method. Preprints, *SPIE Defense and Security Symp., Conf.*
2 *5425: Algorithms and Technologies for Multispectral, Hyperspectral, and Ultraspectral*
3 *Imagery X*, Orlando, FL, Society of Photo-Optical Instrumentation Engineers, 5425–
4 5437.

5 Nutter, P. A., and J. Manobianco, 1999: Evaluation of the 29-km Eta Model. Part I: Objective
6 verification at three selected stations. *Wea. Forecasting*, 14, 5–17.

7 Parrish DF, Derber JC (1992) The National Meteorological Center's spectral statistical
8 interpolation analysis system. *Mon Wea Rev* 20:1747–1763

9 Rabier F, Fourri'e N, Chafa'i D, Prunet P. 2002. Channel selection methods for Infrared
10 Atmospheric Sounding Interferometer radiances. *Q. J. R. Meteorol. Soc.* **128**: 1011–1027.

11 Rodgers CD. 1996. 'Information content and optimisation of high spectral resolution
12 measurements'. pp 136–147 in: *Optical Spectroscopic Techniques and Instrumentation*
13 *for Atmospheric and Space Research II*, SPIE 2380, Hays PB, Wang J (eds).

14 Rodgers CD. 2000. *Inverse Methods for Atmospheres: Theory and Practice*. World Scientific:
15 Singapore.

16 Uddstrom, M., 1991: Forward model errors. Proc. 6th Int. TOVS Study Conference, Airlie,
17 Virginia, Cooperative Institute for Meteorological Satellite Studies, Space Science and
18 Engineering Center, University of Wisconsin, USA, 501–516.

19 Wan, Q. and J Xu, 2011: A numerical study of the rainstorm characteristics of the June 2005
20 flash flood with WRF/GSI data assimilation system over south-east China. *Hydrological*
21 *Processes*, **25**, 1327–1341 (2011) DOI: 10.1002/hyp.7882

22 Weng F., 2007: Advances in Radiative Transfer Modeling in Support of Satellite Data
23 Assimilation. *J. Atmos. Sci.*, **64**, 3799–3807

1 Xu J., S. Rugg, L. Byerle, and Z. Liu, 2009: Weather Forecasts by the WRF-ARW Model with
 2 the GSI Data Assimilation System in the Complex Terrain Areas of Southwest Asia.
 3 *Wea. Forecasting*, **24**, 987–1008.

4 Xu, J and A Powell, 2011: Dynamical Downscaling Precipitation over the Southwest Asian:
 5 Impacts of Radiance Data Assimilation on the Hindcasts of the WRF-ARW Model,
 6 *Atmospheric Research*. doi:10.1016/j.atmosres.2012.03.005

7 Zapotocny, T. H., Jung, J. A., Le Marshall, J. F. and Treadon, R. E. 2008: A Two Season Impact
 8 Study of Four Satellite Data Types and Rawinsonde Data in the NCEP Global Data
 9 Assimilation System. *Wea. Forecast.*,23, 80 – 100.

10 Zhou, H., G´omez-Herna´ndez, J. J., Hendricks Franssen, H.-J., Li, L., 2011. An approach to
 11 handling nongaussianity of parameters and state variables in ensemble kalman filtering.
 12 *Advances in Water Resources*.34 (7), 844–864, DOI: 10.1016/j.advwatres.2011.04.014.

13
14
15

16 **Table 1** The experiment design includes six simulations (EXP1-EXP6)

	Experiment	Description	Initial time
EXP1	CTRL	Control experiment without data assimilation	<u>18 UTC from 30 June to 31 July</u>
EXP2	CON	Conventional data assimilation	<u>00 UTC from 1 to 31 July</u>
EXP3	MW	AMSU-A+MHS data assimilation	<u>00 UTC from 1 to 31 July</u>
EXP4	IR	IASI data assimilation	<u>00 UTC from 1 to 31 July</u>
EXP5	MWIR (MW+IR)	AMSU-A+MHS+IASI data assimilation	<u>00 UTC from 1 to 31 July</u>
EXP6	ALL	Conventional+AMSU-A+MHS+IASI	<u>00 UTC from 1 to 31 July</u>

Formatted Table

	(CON+MW+IR)	data assimilation	
--	-------------	-------------------	--

1
2
3
4
5
6
7

8 **Table2** Listed below are the 279 Channels in IASI corresponding to atmospheric temperature
9 and humidity. The numbers indicate the order in which the channels were chosen in current data
10 assimilation

16	135	226	356	566	1658	2993	3248	3509	5502
38	138	230	360	571	1671	3002	3252	3518	5507
49	141	232	366	573	1786	3008	3256	3527	5509
51	144	236	371	646	1805	3014	3263	3555	5517
55	146	239	373	662	1884	3027	3281	3575	5558
57	148	243	375	668	1991	3029	3303	3577	5988
59	151	246	377	756	2019	3036	3309	3580	5992
61	154	249	379	867	2094	3047	3312	3582	5994
63	157	252	381	906	2119	3049	3322	3586	6003
66	159	254	383	921	2213	3053	3375	3589	
70	161	260	386	1027	2239	3058	3378	3599	
72	163	262	389	1046	2271	3064	3411	3653	
74	167	265	398	1121	2321	3069	3438	3658	
79	170	267	401	1133	2398	3087	3440	3661	
81	173	269	404	1191	2701	3093	3442	4032	
83	176	275	407	1194	2741	3098	3444	5368	
85	180	282	410	1271	2819	3105	3446	5371	
87	185	294	414	1479	2889	3107	3448	5379	
104	187	296	416	1509	2907	3110	3450	5381	
106	193	299	426	1513	2910	3127	3452	5383	
109	199	303	428	1521	2919	3136	3454	5397	

111	205	306	432	1536	2939	3151	3458	5399
113	207	323	434	1574	2944	3160	3467	5401
116	210	327	439	1579	2948	3165	3476	5403
119	212	329	445	1585	2951	3168	3484	5405
122	214	335	457	1587	2958	3175	3491	5455
125	217	345	515	1626	2977	3178	3497	5480
128	219	347	546	1639	2985	3207	3499	5483
131	222	350	552	1643	2988	3228	3504	5485
133	224	354	559	1652	2991	3244	3506	5492

1
2
3
4
5

6 **Caption of Figures**

7 **Fig. 1** Distribution of observations. (a) conventional data on July 1, 2012 with the atmospheric
8 temperature (yellow), moisture (dark blue) and surface pressure(light blue), wind speed
9 (orange). (b) Scan coverage of AMSU-A (light blue), MHS (dark blue) and IASI (red)
10 radiance at 18:00 UTC on July 1, 2012

11 **Fig. 2** Vertical weighting functions for satellite observations as a function of height. (a)
12 AMSUA , (b) MHS , (c) IASI

13 **Fig. 3** The scattering plot between observation minus background [OMB] and observation minus
14 analysis [OMA] in the all data (Conventional+AMSU-A+MHS+IASI) experiement
15 (a: surface pressure, b: atmospheric temperature at the height of 2 meters,
16 c: wind speed at the height of 10 meters) for 1 July 2012

17 **Fig. 4** Bias of the temperature (T) forecasts at (a) surface (SFC), (b) lower troposphere (LT),

1 (c) middle troposphere (MT), (d) upper troposphere (UT), (e) lower stratosphere (LS).

2 Unit: °C. CTRL , CON , MW, IR, MWIR and ALL are defined in Table 1

3 **Fig. 5** Bias profile of the temperature (T) forecasts at (a) 6-h , (b) 30-h, (c) 54-h forecasts.

4 | Unit: °C. Other definitions are the same of Fig. 4. The other definition is same as Fig. 4.

5 **Fig. 6** RMSE of the temperature (T) forecasts at (a) surface (SFC), (b) lower troposphere (LT),

6 (c) middle troposphere (MT), (d) upper troposphere , (e) lower stratosphere. Unit: °C

7 | Other definitions can be found in Table 1. The other definition can be found Table 1.

8 **Fig. 7** The RMSE profile of the temperature forecasts at (a) 6-h , (b) 30-h, (c) 54-h forecasts.

9 | Unit: °C. Other definitions are the same of Fig. 4. The other definition is same as Fig. 4.

10

11 **Fig. 8** The bias of the specific humidity (Q) forecasts at (a) surface (SFC), (b) lower troposphere

12 (LT), (c) middle troposphere (MT), (d) upper troposphere , (e) lower stratosphere. Unit:

13 | g/kg. Other definitions can be found in Table 1. The other definition can be found

14 Table 1.

15 **Fig. 9** Bias profile of the specific humidity forecasts at (a) 6-h , (b) 30-h, (c) 54-h forecasts.

16 | Unit: g/kg. Other definitions are the same of Fig. 4. The other definition is same as Fig. 4.

17 **Fig. 10** The RMSE profile of the specific humidity forecasts at (a) 6-h , (b) 30-h, (c) 54-h

18 | forecasts. Unit: g/kg. Other definitions are the same of Fig. 4. The other definition is

19 same as Fig. 4.

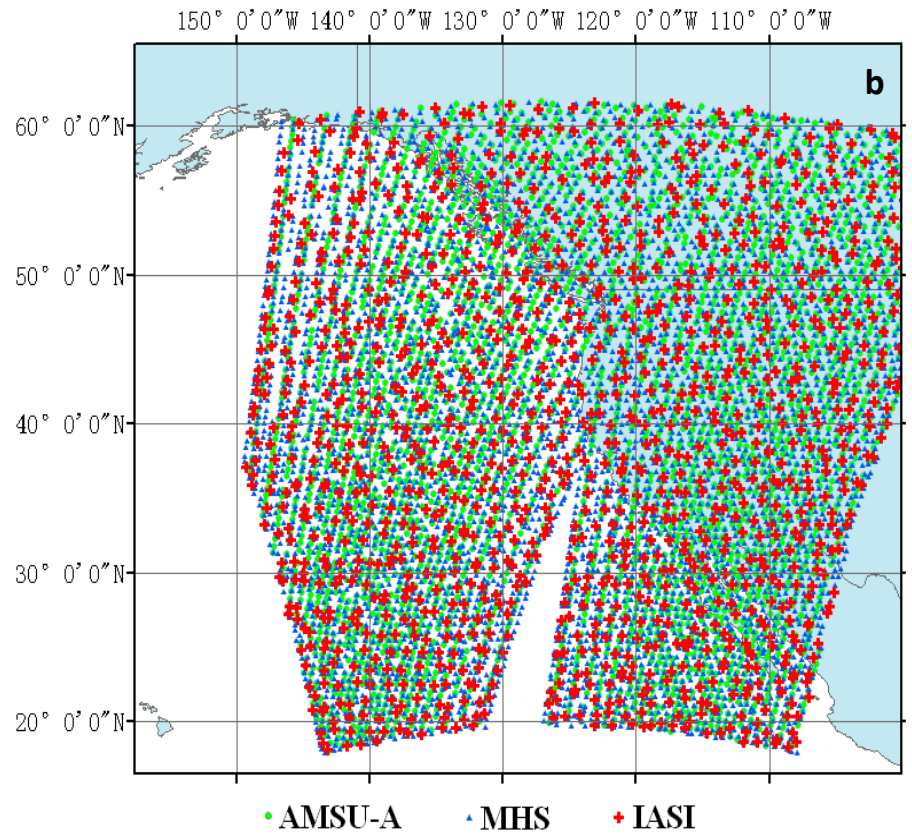
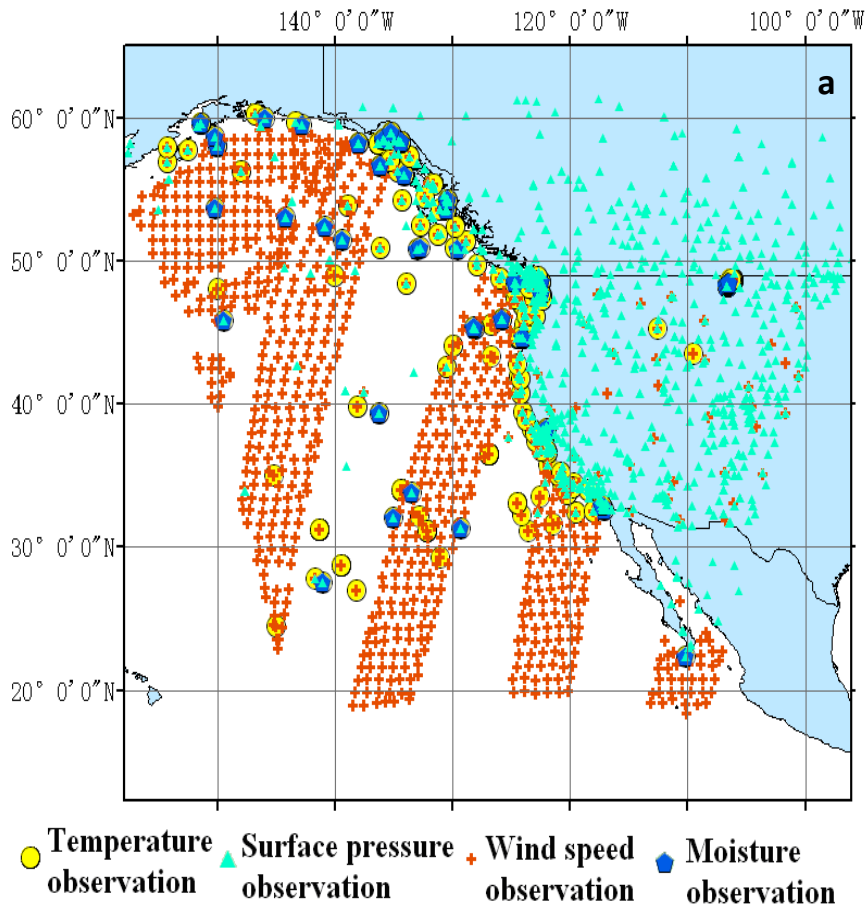


Fig. 1 Distribution of observations. (a) conventional data on July 1, 2012 with the atmospheric temperature (yellow), moisture (dark blue) and surface pressure(light blue), wind speed (orange). (b) Scan coverage of AMSU-A (light blue), MHS (dark blue) and IASI (red) radiance at 18:00 UTC on July 1, 2012

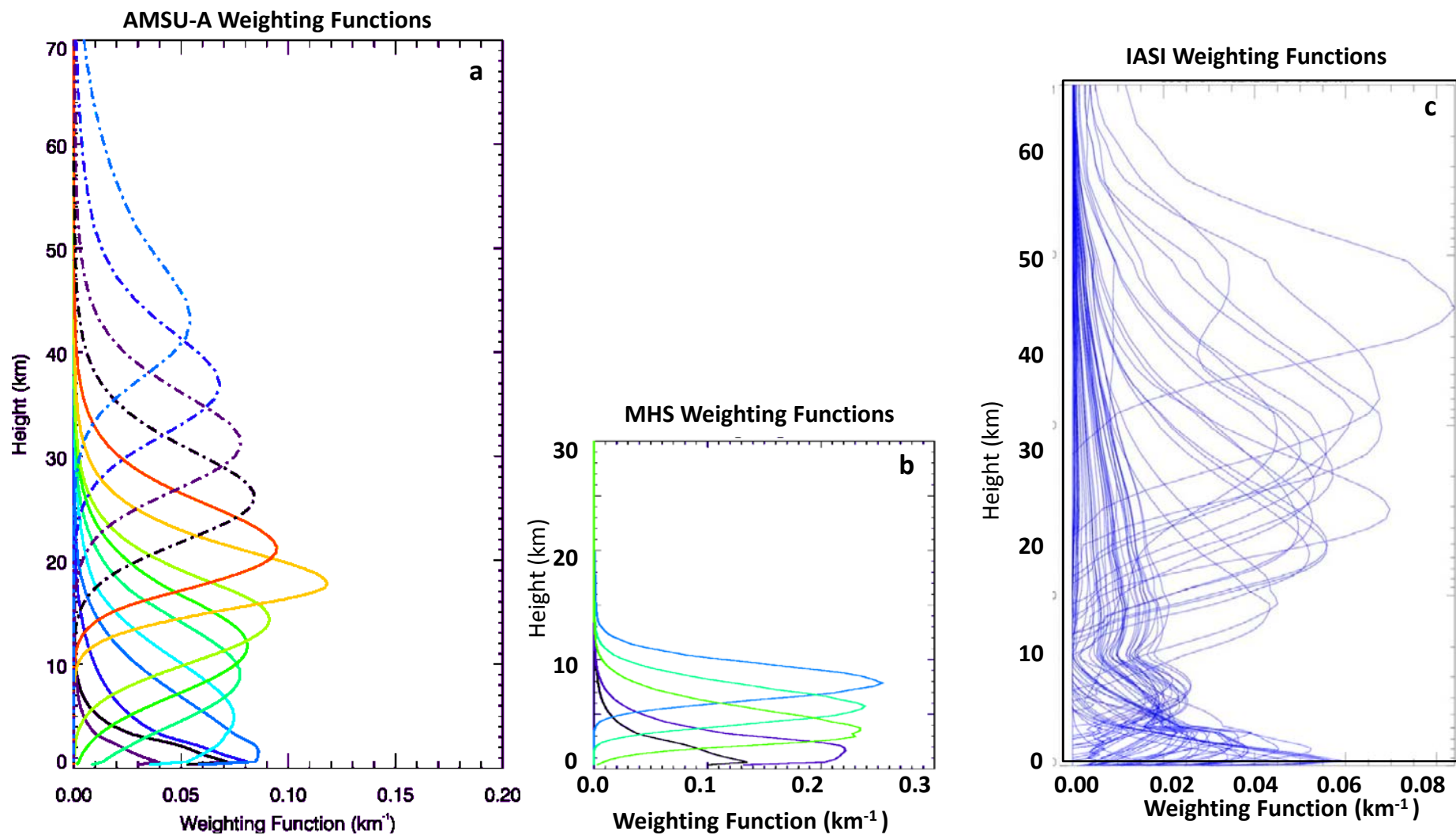


Fig. 2 Vertical weighting functions for satellite observations as a function of height. (a) AMSUA , (b) MHS , (c) IASI

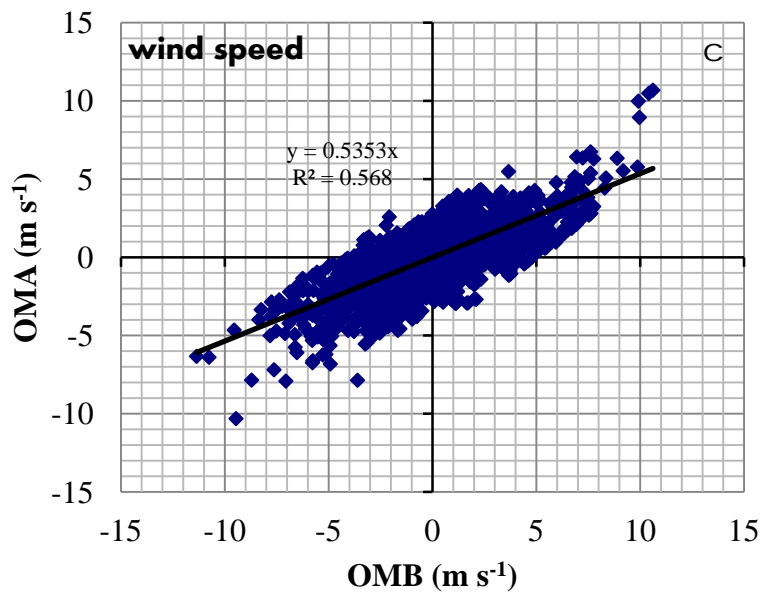
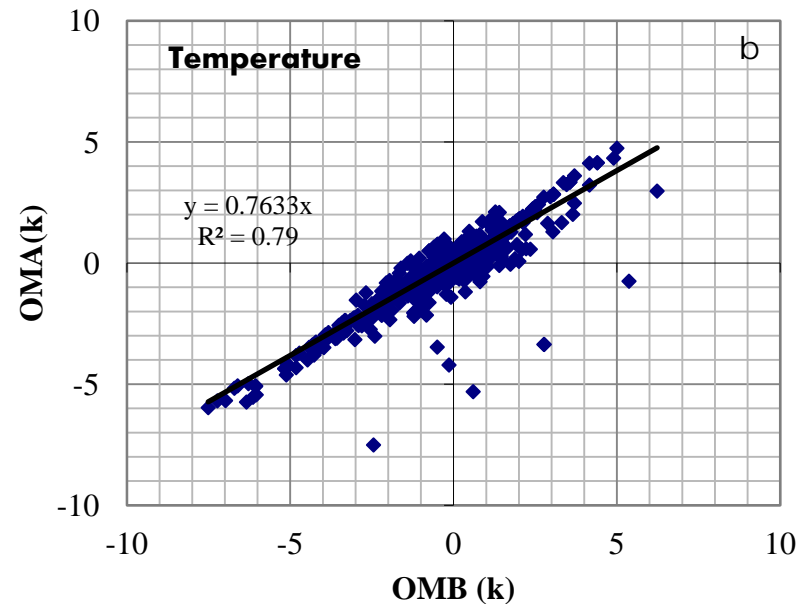
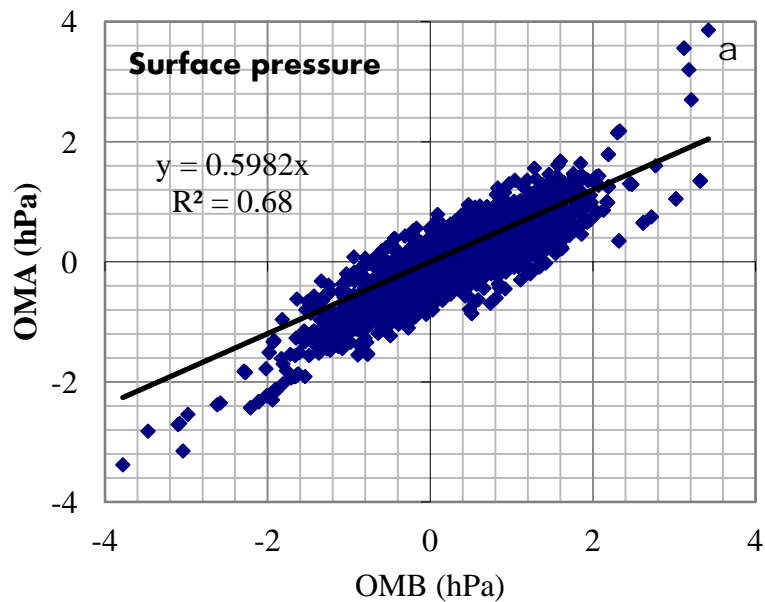


Fig. 3 The scattering plot between observation minus background [OMB] and observation minus analysis [OMA] in the all data (Conventional+AMSU-A+MHS+IASI) **experiment** (a: surface pressure, b: atmospheric temperature at the height of 2 meters, c: wind speed at the height of 10 meters) for 1 July 2012

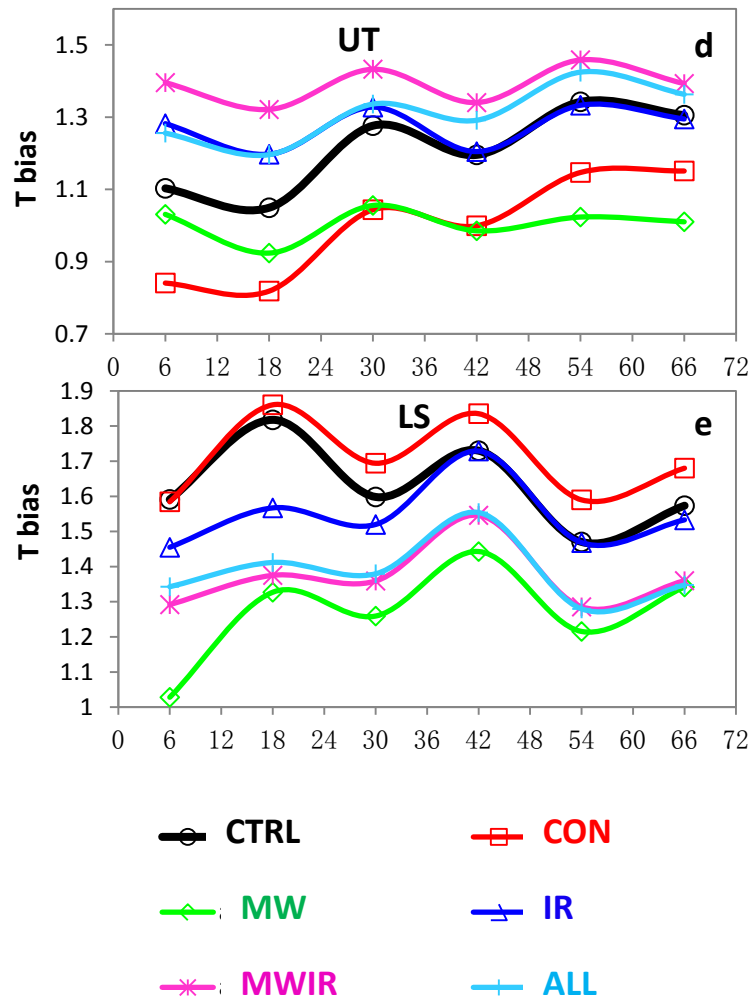
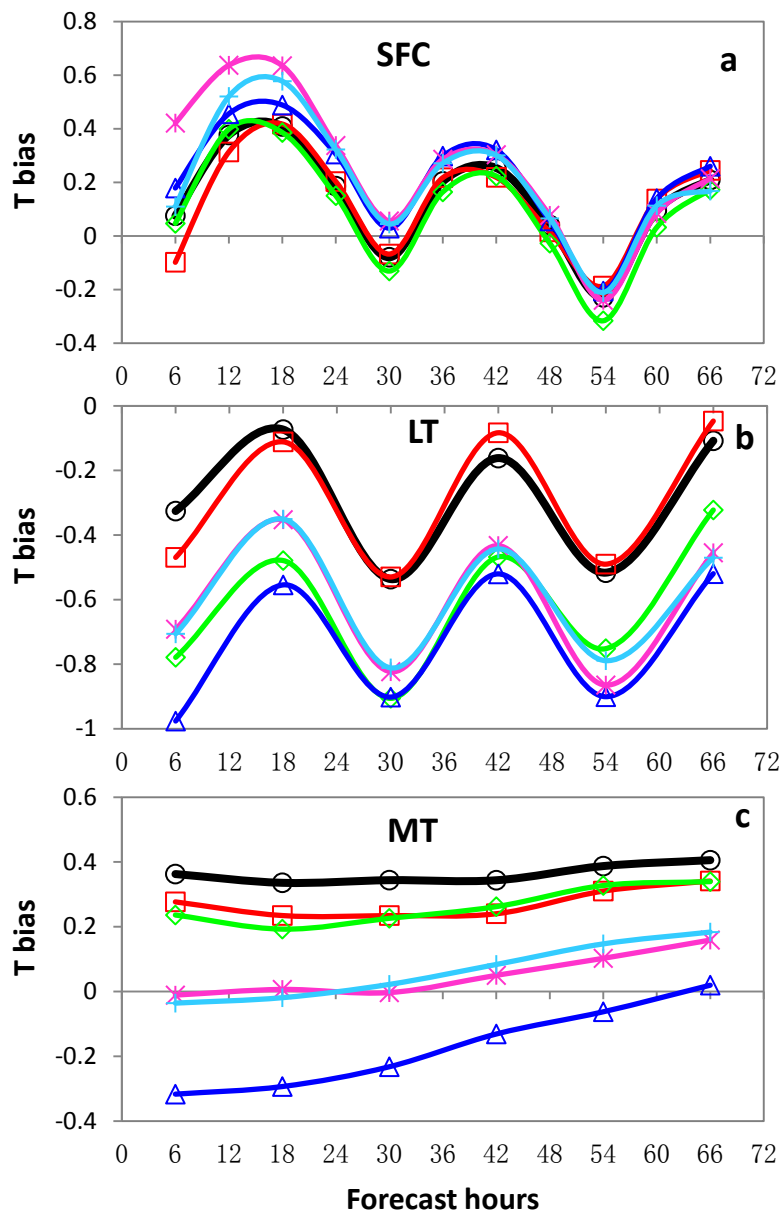


Fig. 4 Bias of the temperature (T) forecasts at (a) surface (SFC), (b) lower troposphere (LT), (c) middle troposphere (MT), (d) upper troposphere (UT), (e) lower stratosphere (LS). Unit: °C. CTRL, CON, MW, IR, MWIR and ALL are defined in Table 1

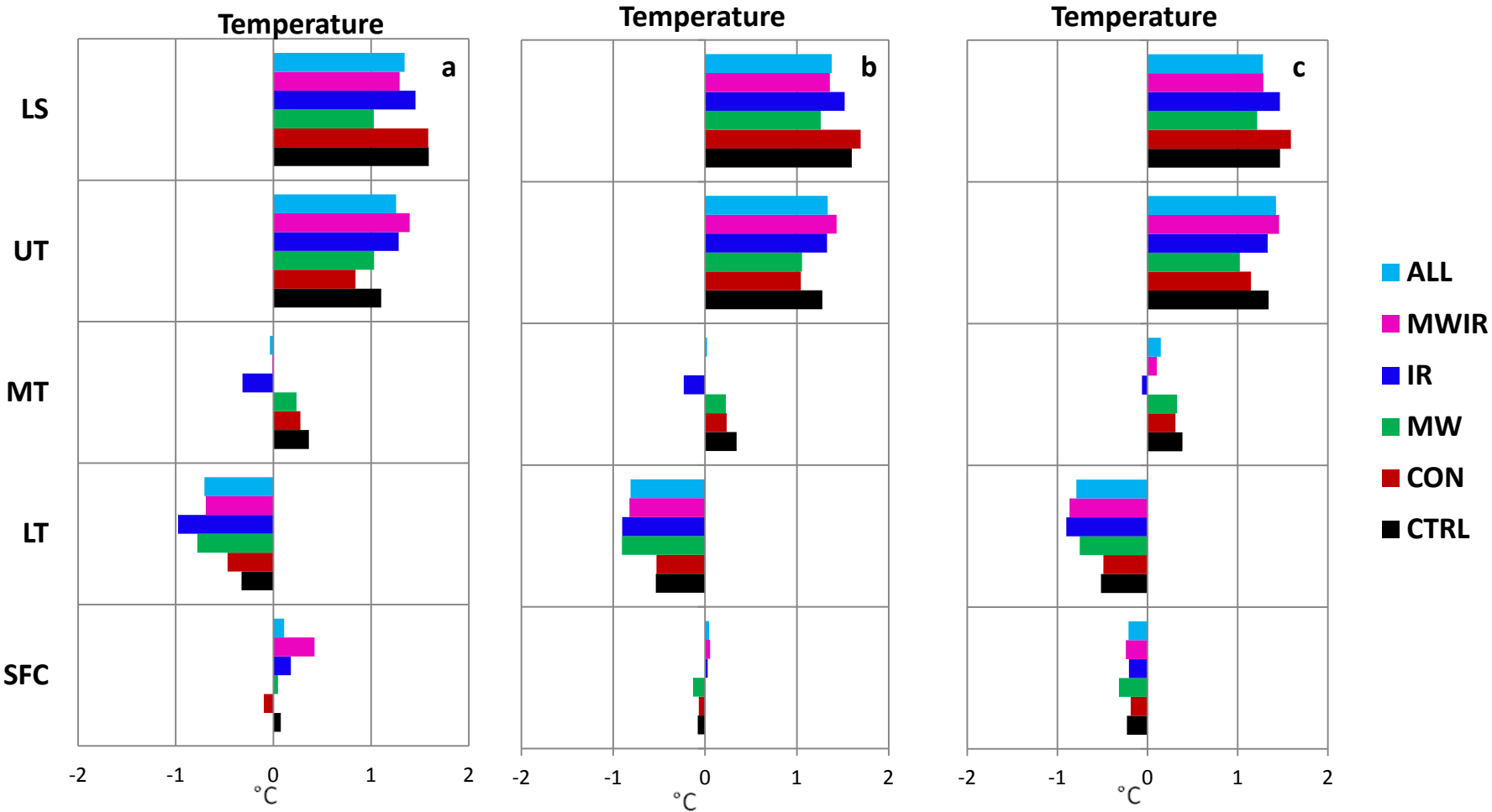


Fig. 5 Bias profile of the temperature (T) forecasts at (a) 6-h , (b) 30-h, (c) 54-h forecasts. Unit: °C. Other definitions are the same of Fig. 4.

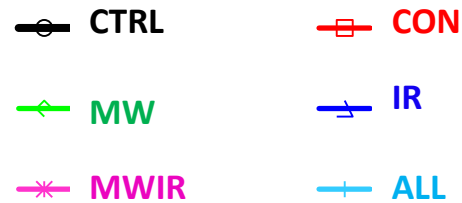
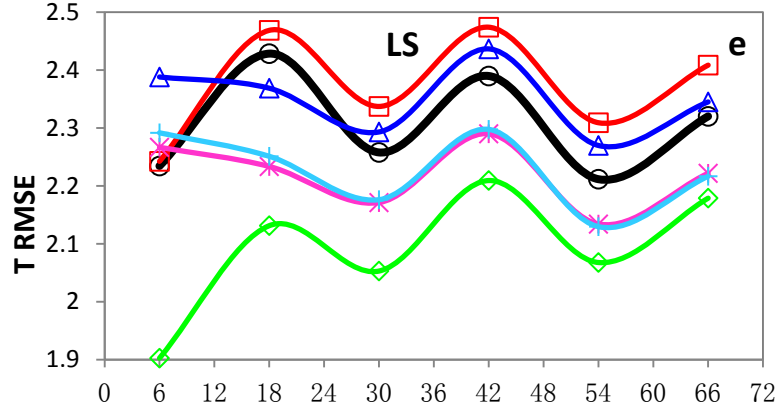
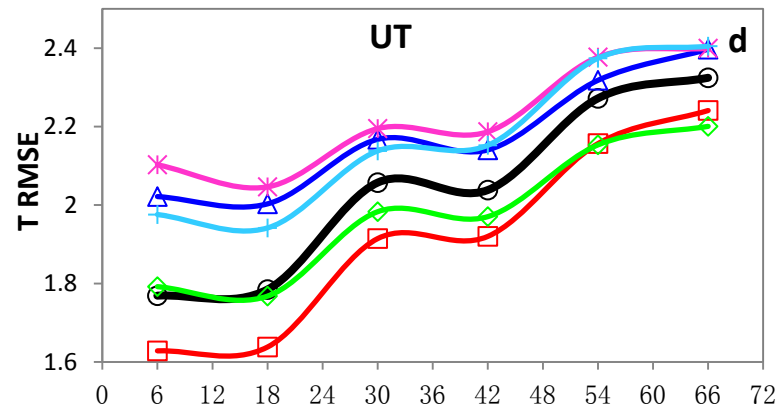
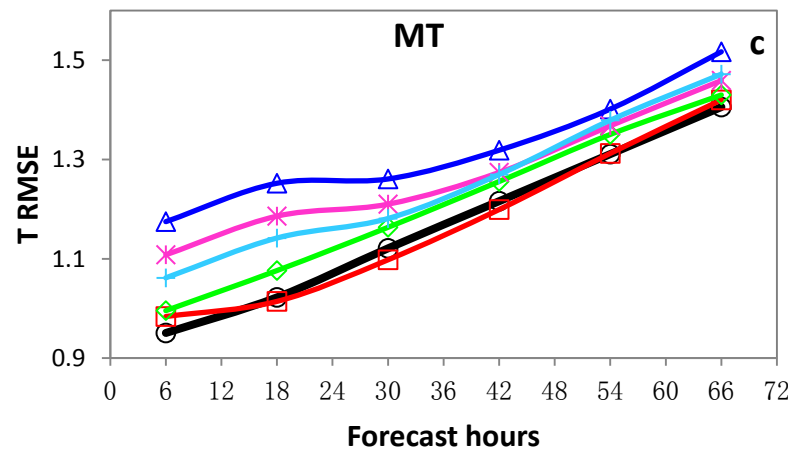
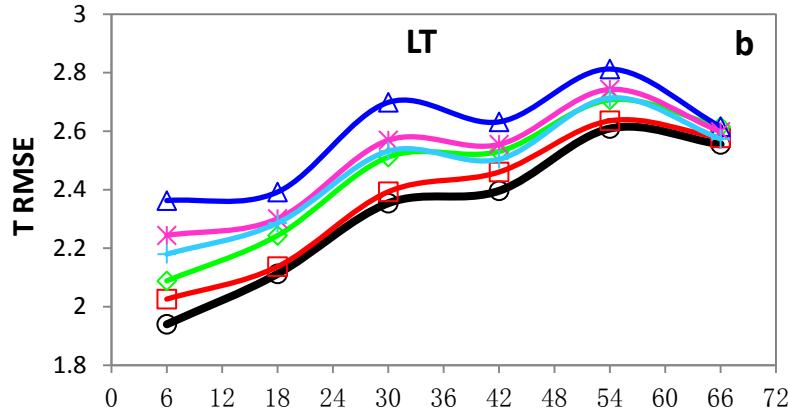
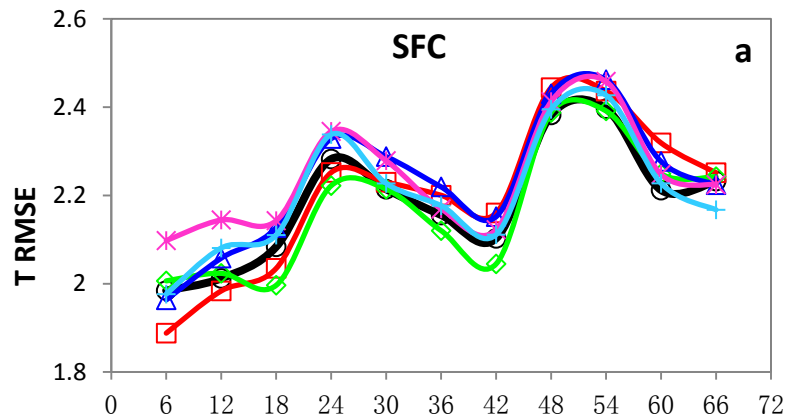


Fig. 6 RMSE of the temperature (T) forecasts at (a) surface (SFC), (b) lower troposphere (LT), (c) middle troposphere (MT), (d) upper troposphere, (e) lower stratosphere. Unit: °C. Other definitions can be found in Table 1.

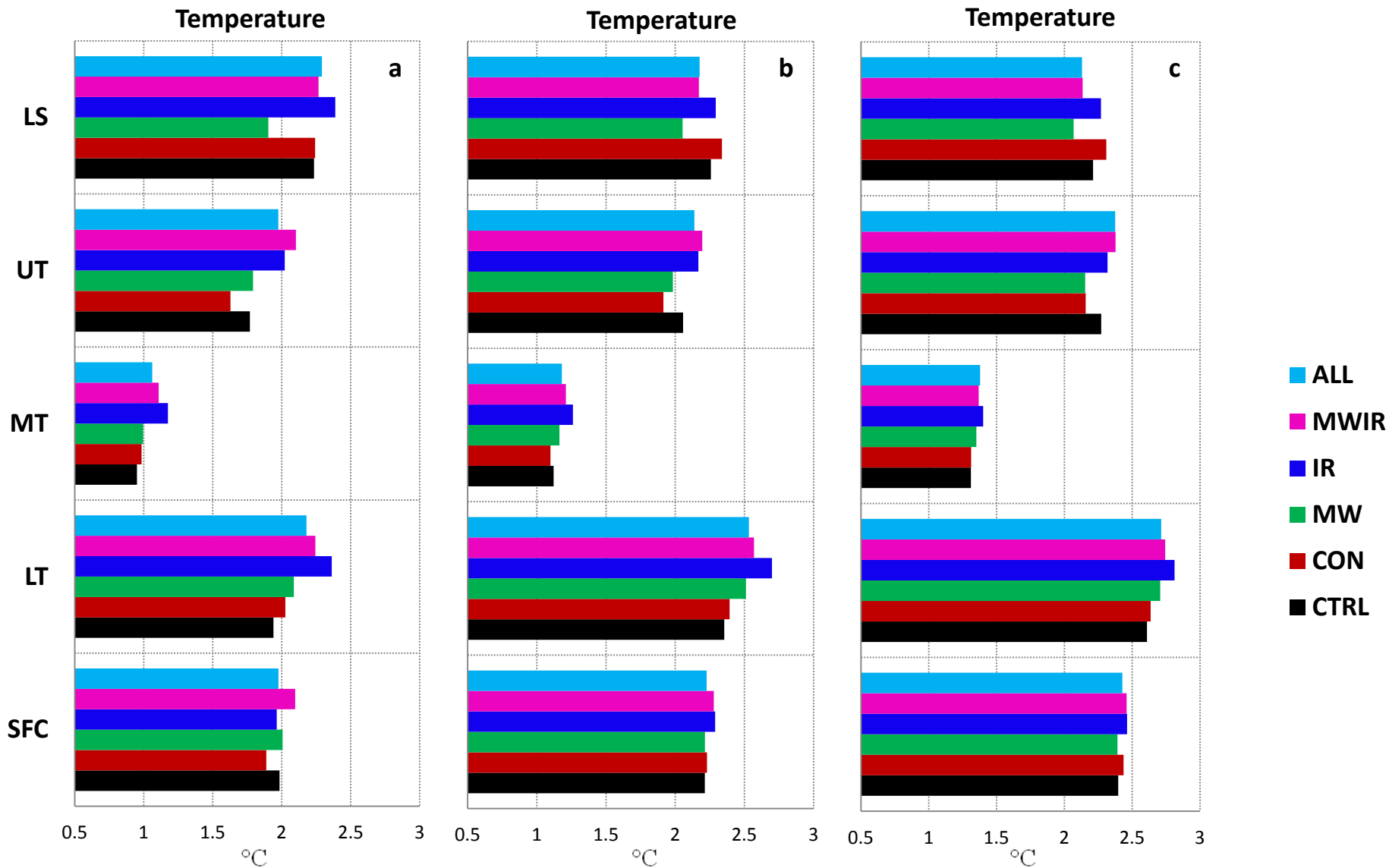


Fig. 7 The RMSE profile of the temperature forecasts at (a) 6-h , (b) 30-h, (c) 54-h forecasts. Unit: °C. Other definitions are the same of Fig. 4.

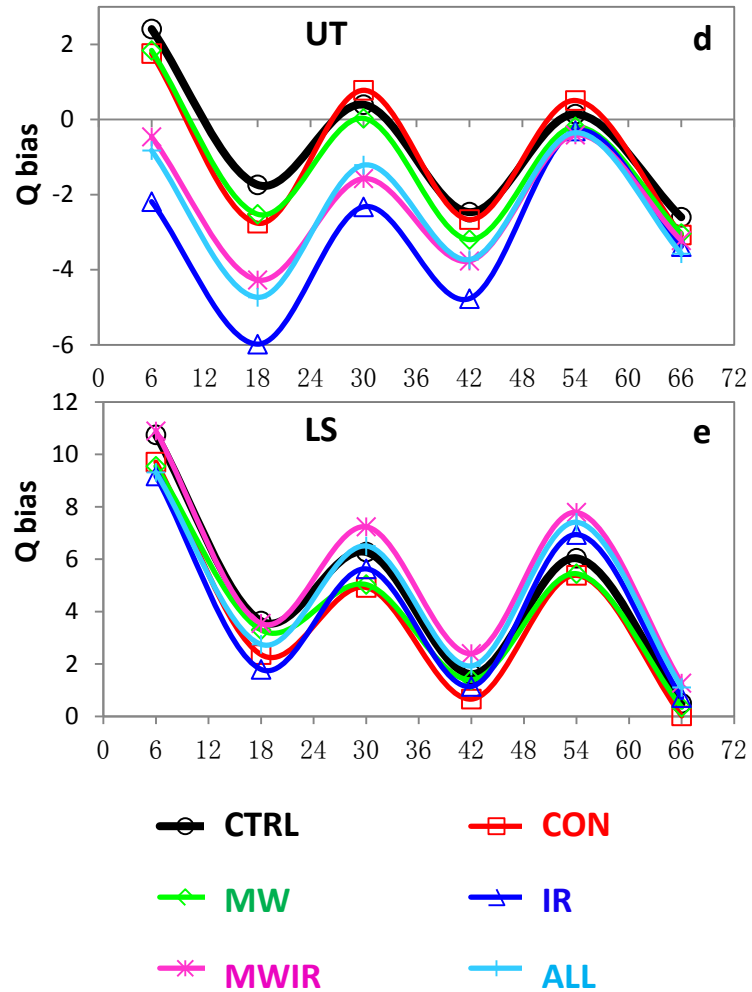
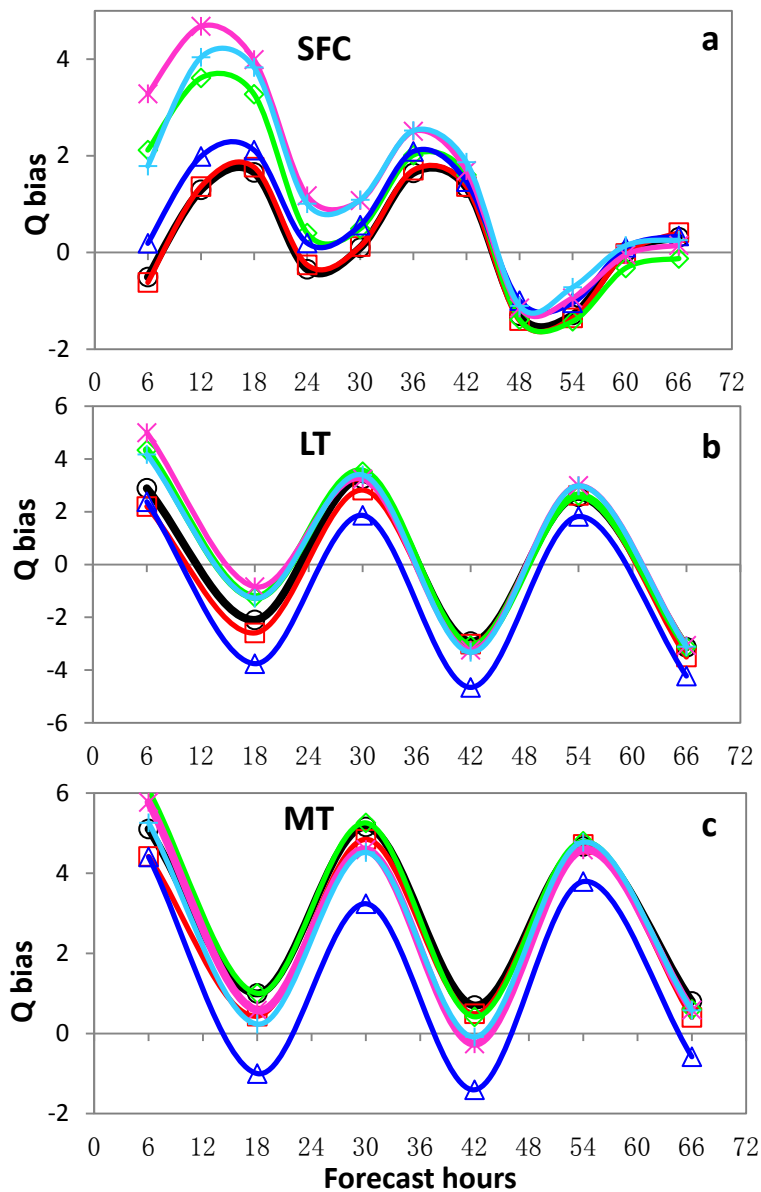


Fig. 8 The bias of the specific humidity (Q) forecasts at (a) surface (SFC), (b) lower troposphere (LT), (c) middle troposphere (MT), (d) upper troposphere, (e) lower stratosphere. Unit: g/kg . Other definitions can be found in Table 1.

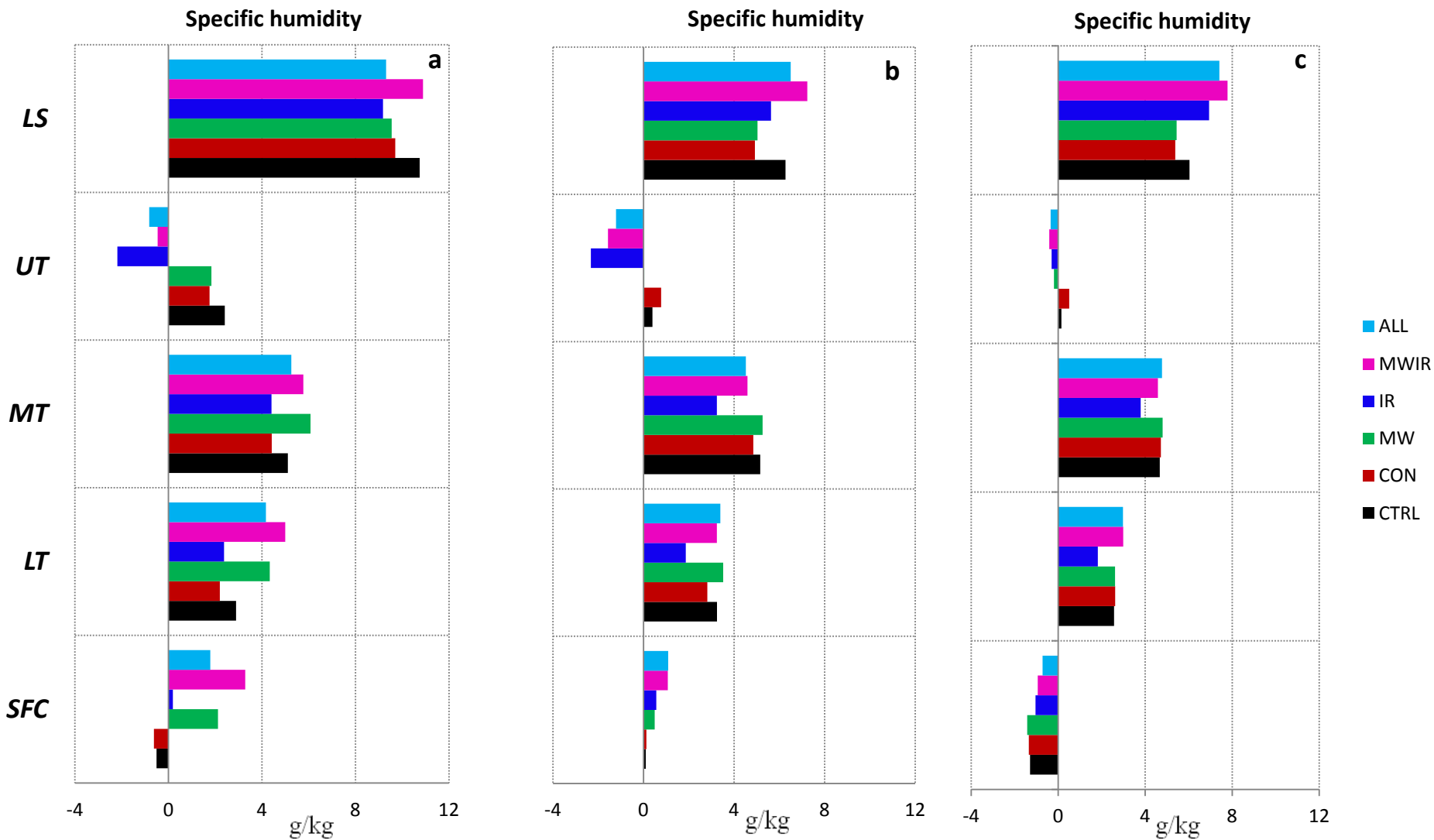


Fig. 9 Bias profile of the specific humidity forecasts at (a) 6-h , (b) 30-h, (c) 54-h forecasts. Unit: g/kg. Other definitions are the same of Fig. 4.

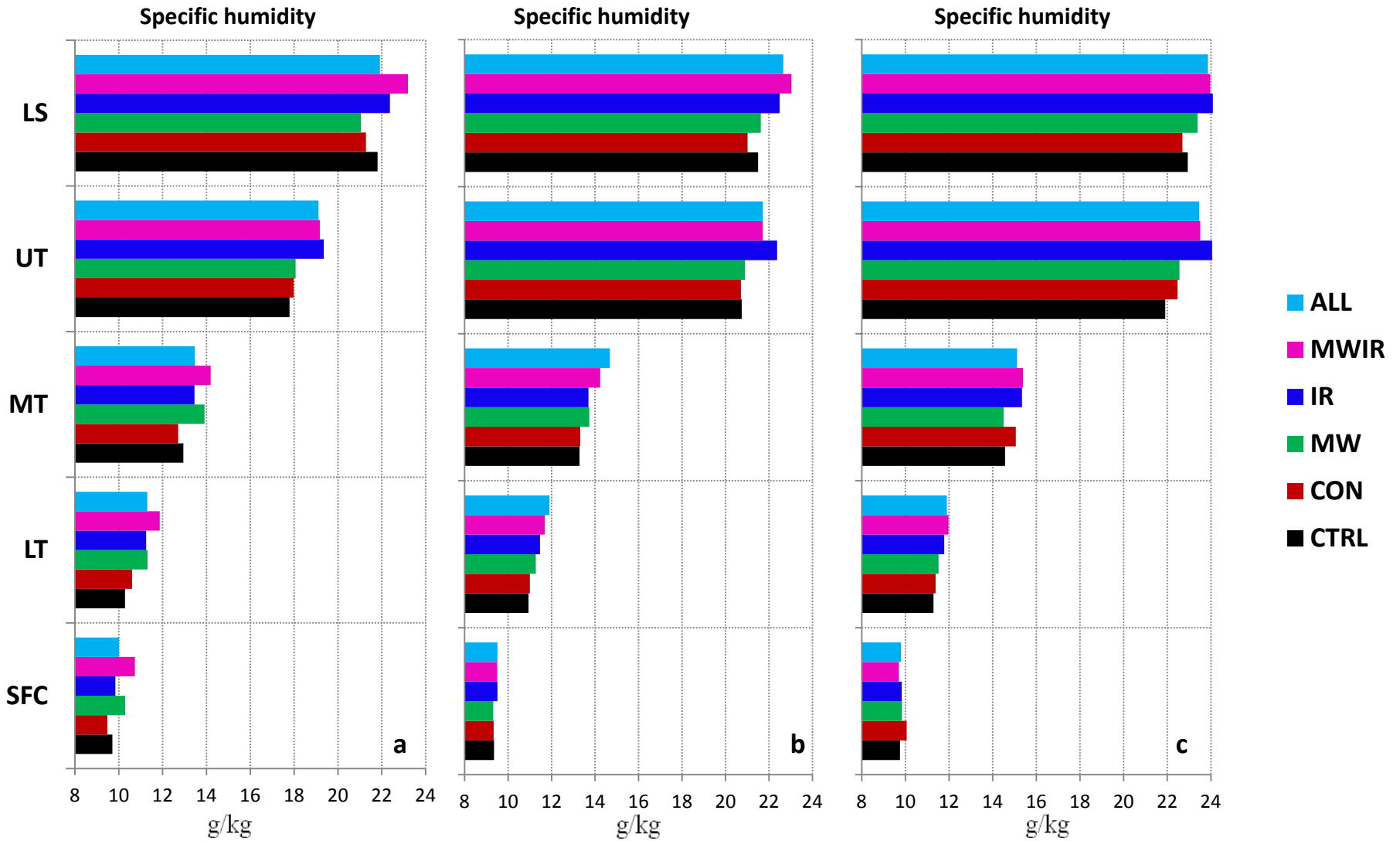


Fig. 10 The RMSE profile of the specific humidity forecasts at (a) 6-h , (b) 30-h, (c) 54-h forecasts. Unit: g/kg. Other definitions are the same of Fig. 4.